

# **Control of chromatic focal shift through wavefront coding**

Hans B. Wach, W. Thomas Cathey  
and Edward R. Dowski, Jr.

## **Abstract**

Control of chromatic aberration through purely optical means is well known. We present a novel optical/digital method of controlling chromatic aberration. The optical/digital system, which incorporates a cubic phase modulation (CPM) plate in the optical system and post processing of the detected image, effectively reduces a system's sensitivity to misfocus in general or axial (longitudinal) chromatic aberration in particular. A fully achromatic imaging system ( one which is corrected for a continuous range of wavelengths ) can be achieved by initially correcting the optical system for lateral chromatic aberration through conventional techniques. Then the axial chromatic aberration is corrected by the inclusion of the CPM plate and post processing.

## **1. Introduction**

In general, optical system design consists of meeting specific requirements under some set of constraints. The constraints of a system vary from application to application. Cost, weight, size, number of optical elements, and materials comprising the optical elements are some typical constraints. Similarly, the performance requirements of a system are application dependent and often times include the minimization of aberrations. Some aberrations may or may not be important or they may be organized into a spectrum of tolerable to intolerable aberrations. Because meeting the system constraints can cause the aberrations to worsen and, conversely, minimizing the aberrations may require breaking the constraints, the challenge lies in making the tradeoff between the two. For example, the design of a digital color imaging system which uses only plastic optical elements is a nontrivial task. While plastic is a desirable material due to its low cost, ease of manufacturing, light weight and durability, it may greatly increase the difficulty in correcting chromatic aberration [1].

In general, color imaging is achieved by taking three greyscale images, either spatially or temporally, with red, green and blue optical filters and combining these images to create a single color image. A color imaging system is susceptible to chromatic aberration due to the wavelength-dependent index of refraction of lenses. This results in three channels of data that are misfocused relative to each other, thereby creating unwanted chromatic effects in the final color images. Existing methods for achromatism have limitations and may not meet the desired constraints.

Chromatic aberration is often avoided by the use of achromatic doublets which are made by placing positive and negative lenses of different refractive indices in contact. In general, one wants to satisfy the relations [2]

$$\begin{aligned}\frac{K_1}{V_1} + \frac{K_2}{V_2} &= 0 \\ K_1 + K_2 &= K\end{aligned}\tag{1}$$

where  $K_i$  is the power (inverse focal length) of the  $i^{\text{th}}$  lens,  $K$  is the system power,  $V_i$  is its Abbe number (which is a measure of index change with wavelength) and the thin lens approximation is employed. While this method is useful, it is limited in that it only corrects for two wavelengths. Although it is possible to create apochromatic doublets which correct for three distinct wavelengths, these are rare because they are typically made with crystalline materials which do not polish well and are not chemically stable [2].

Apochromatic triplets are more common and require three different materials for the lenses. Again the limitation is that only three wavelengths will be corrected for, while the others are left uncorrected.

Notice that, in general, to correct for more wavelengths, more materials must be introduced which may be considered a limitation. There are special cases, however, in which it is possible to create lens systems with a single material which corrects two wavelengths for either the axial (longitudinal) or lateral (magnification) chromatic aberration (see appendix A1 for a description of these) but not both simultaneously [3],[4].

Chromatic aberration can also be corrected through the use of hybrid refractive-diffractive elements. Whereas refractive optics have a decreasing index of refraction with increasing wavelength, diffractive optics have the opposite relation. This difference allows diffractive elements to have negative Abbe numbers. In addition the magnitude of the Abbe numbers are much smaller than those of refractive elements. These small Abbe numbers allow the powers of the individual elements to be reduced. Although this provides another option in satisfying the relation in (1), these systems also have limitations in that they cannot correct for both types of chromatic aberration [5], [6] and [7].

In this paper, a system is designed for color imaging which is fully achromatic. It is an example of the simplifications that can be achieved in optical system design where control of chromatic aberration is important. Through the addition of a special optical element, or a modification of an existing surface, and digital post processing of the acquired image, this hybrid optical-digital system corrects for chromatic aberration over a large range of wavelengths.

The rest of the paper proceeds as follows. Section 2 provides a brief review of chromatic aberration, the associated radian misfocus parameter is defined, and some aberrated point spread functions (PSFs) are shown. Section 3 describes what we call the traditional system with chromatic aberration and shows, mathematically, the dependence of the PSF on wavelength. Then the CPM system is illustrated in Section 4 and a description of the digital filter design is given. Finally, Section 5 compares the results obtained with the two systems and Section 6 presents concluding remarks.

## **2. Chromatic Aberration**

Chromatic aberration is simply caused by the dependence of refractive index on wavelength.

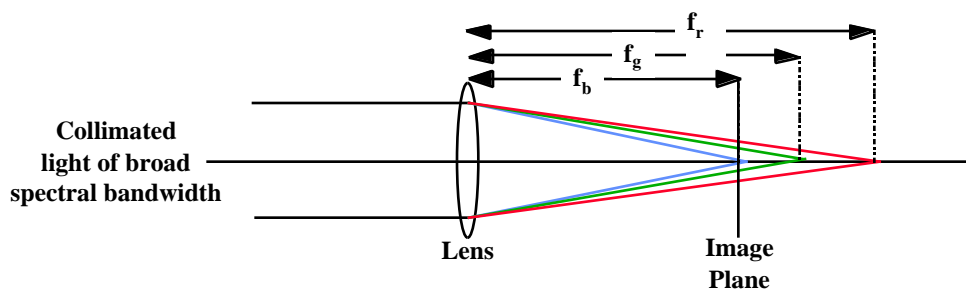


**Figure 1.** Demonstrating axial chromatic aberration with a single lens. The distances  $f_r$ ,  $f_g$  and  $f_b$  are the focal lengths for red, green and blue light.

Figure 1 shows how collimated red, green and blue light passing through a singlet will focus at different positions along the optic axis. This type of aberration is called axial

(longitudinal) chromatic aberration. With an image plane at a fixed distance from the lens, the three images will be misfocused relative to each other. For the case of Figure 1, the image plane is placed at a distance where blue light is in focus. In a traditional system the image distance can be defined by

$$\frac{1}{d_i} = \frac{1}{f} - \frac{1}{d_o} \quad (2)$$

For a fixed object distance,  $d_o$ , this system will focus at the same image distance,  $d_i$ , given a fixed focal length,  $f$ . However, consider that the focal length changes with wavelength,  $\lambda$ , as

$$\frac{1}{f} = (n(\lambda) - 1) \left( \frac{1}{R_1} - \frac{1}{R_2} \right) \quad (3)$$

where  $R_1$  and  $R_2$  are the radii of curvature of the two surfaces of the lens and  $n(\lambda)$  is the wavelength dependent index of refraction of the material. Now the image distance may be written as a function of wavelength

$$d_i(\lambda) = \frac{1}{f(\lambda) - \frac{1}{d_o}} \quad (4)$$

It is obvious from (3), (4) and Figure 1 that the PSF of the system will be non-ideal. One in-focus point of blue light (Figure 2.d) and two increasingly out-of-focus green (Figure 2.c) and red (Figure 2.b) points would appear at the image plane thereby producing the undesired composite PSF shown in Figure 2.a. The amount of misfocus can be characterized by the radian misfocus parameter,  $\delta$ , which is given by [9]

$$= \frac{L^2}{4} \left( \frac{1}{f(\lambda)} - \frac{1}{d_o} - \frac{1}{d_{ccd}} \right) = 2 W_{020}, \quad (5)$$

where  $L$  is the one-dimensional length of the lens aperture. The distance  $d_o$  is measured between the object and the first principal plane of the lens, and  $d_{ccd}$  is the distance between the second principal plane and the CCD detector. The function  $f(\lambda)$  is the focal length of the lens. It is now obvious that with a fixed  $d_o$  and  $d_{ccd}$  that a particular choice of  $\lambda$  (corresponding to blue light in this case) will give a  $f(\lambda)$  that satisfies the imaging relation, therefore making  $W_{020} = 0$ .

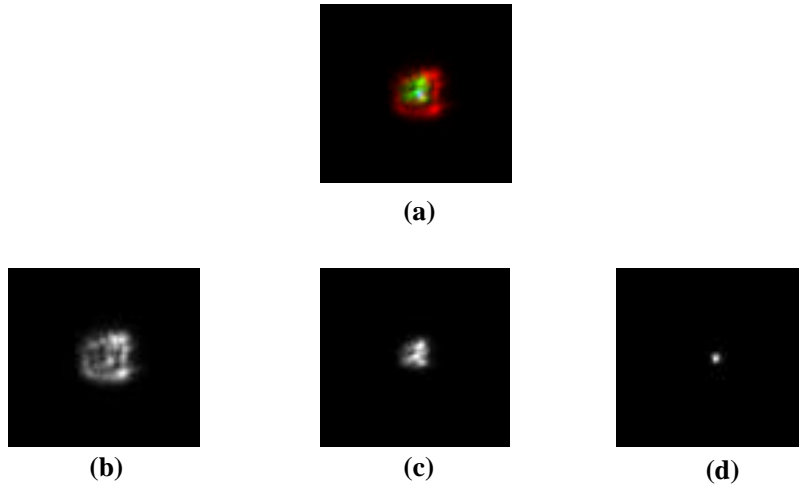


**Figure 2.** Experimentally acquired point spread functions from a chromatically aberrated system. The composite PSF is shown in (a). Also shown is the red PSF (b), green PSF (c) and the blue PSF (d).

Figure 2 shows measured PSFs from an axial chromatic aberrated system where blue light was focused at a fixed image plane (Figure 2.d). While all of the blue information in a scene was well preserved, the other two channels of data were severely out of focus (Figures 2.b and 2.c), thus deteriorating the quality of the final color image (Figure 2.a).

Lateral (field, off-axis or magnification) chromatic aberration may also plague the imaging quality of an imaging system. Here, while the images all focus at the same plane, the red, green and blue images have different sizes due to the wavelength dependent

magnification. As stated in the introduction, purely optical means exist to correct this type of chromatic aberration. The trivial symmetric system or the Huygen's ocular are two such systems which correct lateral chromatic aberration.

### 3. Traditional System

A system (shown in Figure 3) was designed with two glass singlets, a rectangular aperture, red, green and blue optical filters, and a CCD camera. The system was designed to have almost solely axial (longitudinal) chromatic aberration relative to other aberrations. A ray intercept curve for the system, shown in Figure 4, demonstrates this. Having a narrow field of view, the system does not suffer a great deal from field dependent aberrations. The high magnification of the system is good for illustrative purposes as it accentuates the chromatic aberration.

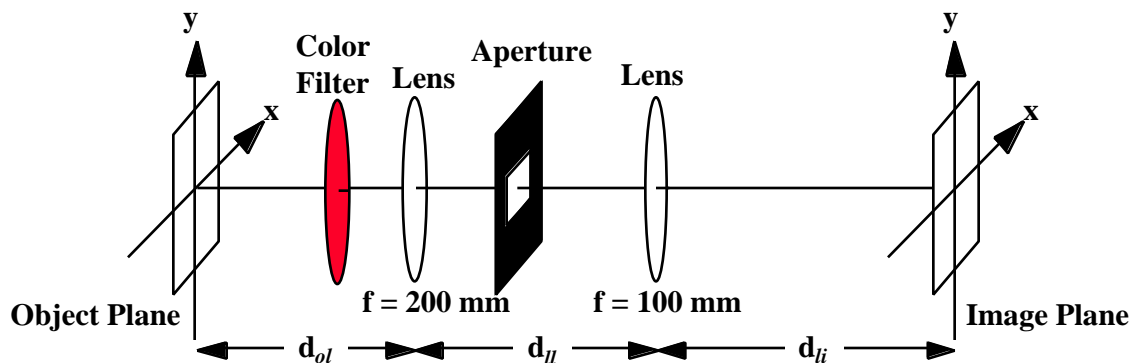


**Figure 3.** A traditional optical system consisting of two singlets, a clear rectangular aperture, red, green and blue color filters and a CCD at the image plane.

The distances  $d_{ol} = 250\text{mm}$ ,  $d_{ll} = 43\text{mm}$ , and  $d_{li} = 87\text{mm}$  are all fixed, giving the system a working  $f/\#$  of 11.7 and an effective focal length of 78.5mm. Recall, that the system was designed so that blue light would focus properly at the image plane. This can be seen from the ray intercept curve in Figure 4.

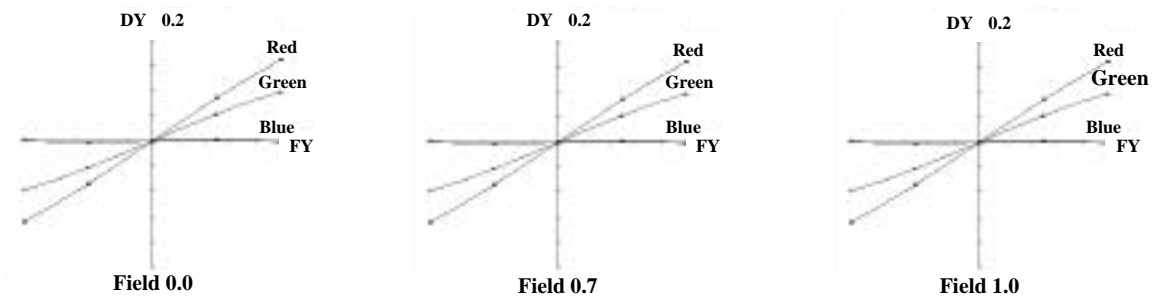


**Figure 4.** The ray intercept curve for the system shown in Figure 3. Here FY is the ray height at the exit pupil and DY is the height at which a ray crosses the image plane. The three graphs are for a point at full field, 0.7 full field and an on axis.

The ray intercept curves in Figure 4 are a graphical way of showing ray height at the image plane (DY) as a function of their height at the exit pupil (FY) from a particular field location (from on axis to full field). The shape of the plots are the derivative of the pupil dependent aberrations. Since there is almost no change in the curves at different field locations, it is obvious, from Figure 4, that there are relatively no field dependent aberrations. Notice also that axial misfocus as a function of color is the dominant aberration present as the curves are all roughly linear.

In order to get a color image, three successive images were taken using three color filters. While this method required the CCD and the object to have no relative movement, it gave full resolution in each channel, thus reducing color aliasing and isolating chromatic aberration.

The system can be modeled as a single-lens system with the rectangular aperture right at the lens and the generalized pupil function can be written

$$\mathbf{P}(x, y) = P(x, y)\exp[j \quad (x^2 + y^2)] \quad (6)$$

where  $P(x, y) = \text{rect}(\frac{x}{L})\text{rect}(\frac{y}{L})$  and is dependent on as given in (5). A calculation of the optical transfer function (OTF) gives an expression which is dependent on and

therefore dependent on the wavelength,  $\lambda$ . Due to rectangular separability the OTF can be calculated in one dimension to give

$$H(f_x, \lambda) = \frac{f_x}{2f_0} \text{sinc} 2 \left| \frac{f_x}{f_0} \right| - \frac{f_x}{f_0} \quad (7)$$

where  $f_x$  denotes spatial frequency,  $f_0 = \frac{L}{2d_i}$  and

$$sinc(x) = \begin{cases} 1 - |x|, & |x| \leq 1 \\ 0, & \text{otherwise} \end{cases}$$

This result is reached in [8].

#### 4. Cubic Phase Modulation Plate System

A new system was designed which is identical to the traditional optical system shown in Figure 3 but has a cubic phase modulation plate at the aperture stop. This system is shown in Figure 5. The CPM plate is a transparent optical element with a cubic phase profile. It can be fabricated by grinding the surface on glass or plastic directly or, for high volume, an ultra precision mold insert can be machined. The CPM plates can then be mass produced with an injection molding process. A surface plot of the plate is shown in Figure 6.

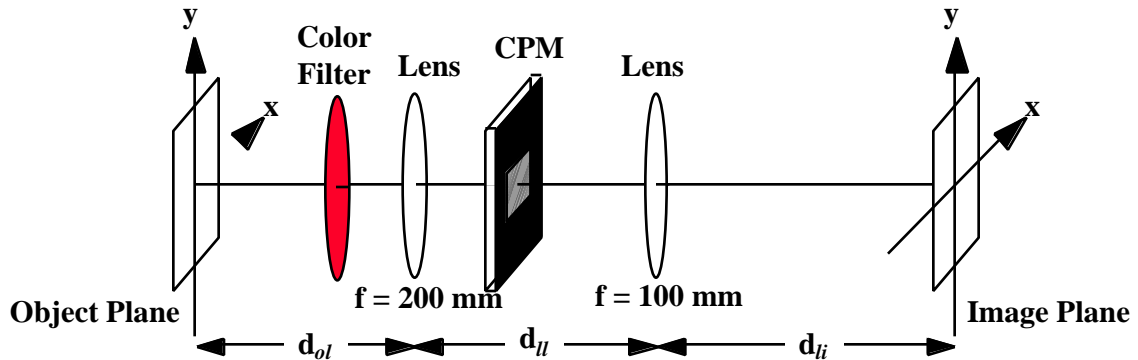


**Figure 5.** CPM system consisting of two singlets, a clear rectangular aperture, CPM plate, red, green and blue color filters and a CCD at the image plane.

Notice that the mask is asymmetrical and rectangularly separable which can be seen from the phase function

$$\exp[j \phi(x, y)], \text{ where } \phi(x, y) = \alpha(x^3 + y^3) \quad (8)$$

where  $\alpha$  is a constant that determines the maximum phase deviation. With the plate placed at the aperture stop, the generalized pupil function becomes

$$\mathbf{P}(x, y) = P(x, y)\exp[j \alpha(x^2 + y^2)]\exp[j \phi(x, y)] \quad (9)$$

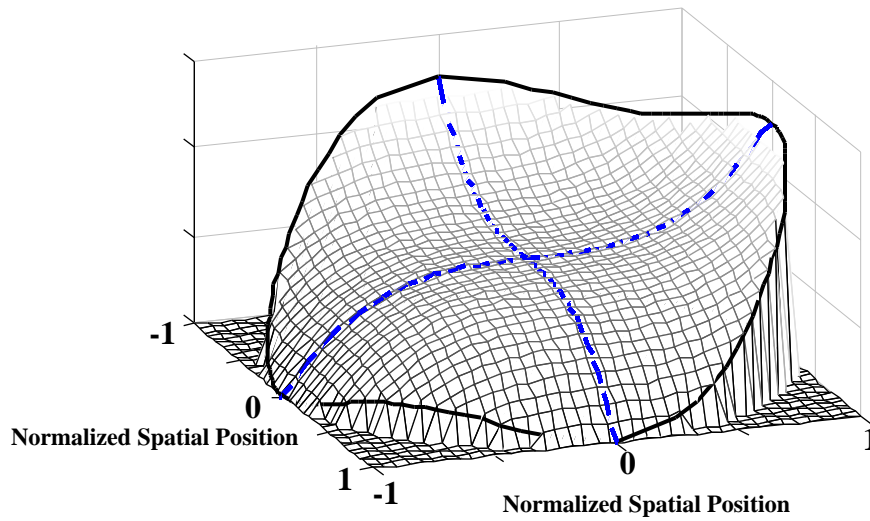


**Figure 6.** Surface plot of cubic phase modulation (CPM) plate with a phase function  $\phi = \alpha(x^3 + y^3)$  with  $\alpha = 20$ ,  $|x| \leq 1$  and  $|y| \leq 1$ .

Again, the OTF can be calculated in one dimension due to rectangular separability, but this time the calculation benefits by the use of Woodward's Ambiguity function [10] and an approximation through the method of stationary phase. The expression, derived in [9], can be written as

$$H(f_x, \dots) = \left| \frac{1}{12 f_x L^2} \right|^{1/2} \exp[j(\dots(x_i) + 2 f_x \dots x_i \pm \dots/4)] \quad (10)$$

$$\text{where } \dots(x) = [(x + f_x/2)^3 - (x - f_x/2)^3]$$

$$\text{and } x_i = \frac{\dots}{3 f_x}$$

The OTF given in (10) has two very interesting features. First, notice that the magnitude of the OTF is independent of the misfocus parameter,  $\dots$ , and therefore independent of the wavelength of light,  $\dots$ . The PSF, while not directly ideal for imaging, is also independent of wavelength, as is the step response. The second interesting feature of the OTF is that it has no zeros and reconstruction at all frequencies, therefore, is possible. In order to get an ideal PSF or step response for the combination optical and digital system, digital post processing is required on the images. Therefore some characterization of the system is necessary.

In order to create a digital filter, the response of the system to some input must be simulated or measured to characterize the system. Because the system behaves nearly identically at all wavelengths, only a single digital filter is needed for all images. While the response to a point of light at the object plane (PSF) will characterize the system in an ideal case, it will fall short of correctly characterizing the system in the case where the resolution is limited by the pixel size in the CCD detector. That is, the measured PSFs with the CPM system have high frequencies that cannot be detected by the CCD and aliasing corrupts the measurement. A more accurate characterization of the system can be made by measuring or simulating the step response,  $v(x)$ , which is linearly related to the PSF,  $h(x)$ , by

$$v(x) = \int h(x)u(x - x)dx = h(x)* u(x) \quad (11)$$

where \* denotes convolution and  $u(x)$  is the unit step defined as,

$$u(x) = \begin{cases} 1, & x \geq 0 \\ 0, & \text{otherwise} \end{cases}$$

The magnitude of the spatial frequency spectrum falls off inversely with spatial frequency. Therefore, this signal has a lower bandwidth than the PSF, thus reducing the aliasing effect.

The ideal step response,  $v'$ , is calculated using the ideal, incoherent PSF for  $h(x)$  and substituting this into (11). Here, the ideal incoherent PSF is taken to be a  $\text{sinc}^2(\bullet)$ . Now with an ideal target response,  $v'$ , and a measured response,  $v$ , the filter,  $f$ , can be calculated by solving a series of linear equations

$$Hf = v \tag{12}$$

where H is a convolution matrix made from the measured step response,  $v$ . The least squares solution to (12) is found to be

$$f = (H^T H)^{-1} H^T v \tag{13}$$

This idea can be expanded to find a single filter which can be used on all images regardless of wavelength. The result is a 1-D filter that can be applied to (convolved with) the rows and columns of the intermediate image due to the rectangular separability. The filter depends on the optical system, the desired image quality and time requirements. The filter must be at least as long as the impulse response of the optical system which, in turn, depends on the maximum phase deviation of the CPM plate. Therefore, the filter length and frequency response can be fashioned to give the best performance.

## **5. Results and Comparisons**

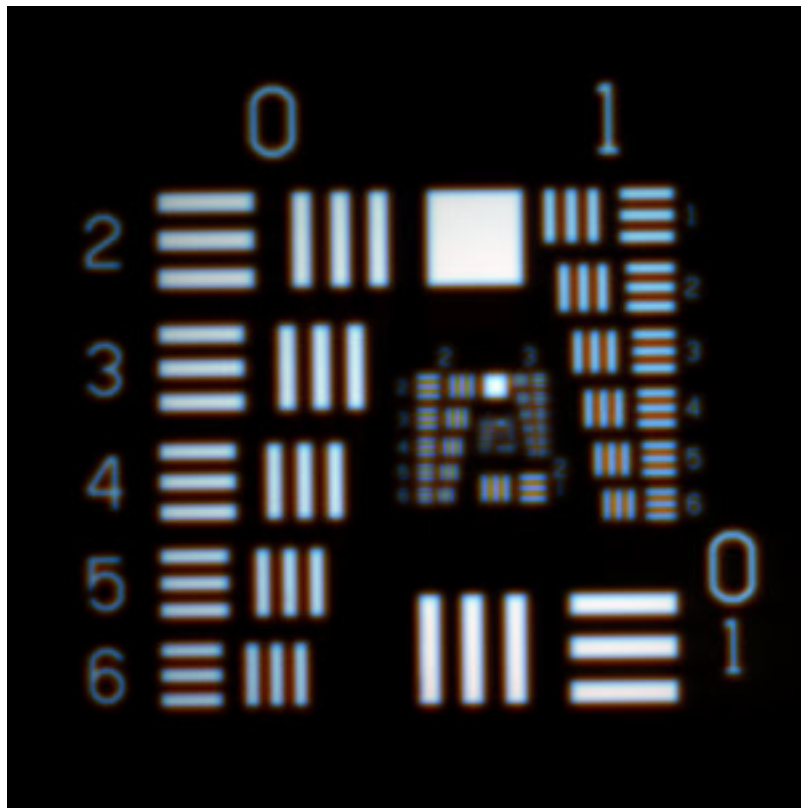
A chrome-on-glass Air Force resolution target was used as the object. This object was illuminated from the back with diffuse white light. By acquiring and combining three sequential images with three different optical color filters, color images were taken with both systems. In the traditional system, while the blue image was in focus, the green and red image had misfocus parameters of  $g=27$  (about 4 waves of misfocus) and  $r=34$  (about 5 waves of misfocus) respectively. These severe misfoci greatly reduced the quality of the image and rendered the image useless. However, with the simple modification to the optical system, described in Section 4, and some post processing, a very high quality image was produced. A comparison of the two systems can be seen in Figures 7, 8 and 9.

The image in Figure 7.a was acquired with the traditional system and shows the effect of chromatic aberration through the loss of resolution and the color effects. In comparison, the image of Figure 7.b shows the image acquired with the CPM system. Notice that this image is truly black and white (as it should be) and has a much higher resolution than the traditional system. It is interesting to zoom into the sub-target at the center portion of the image, as shown in Figure 8.

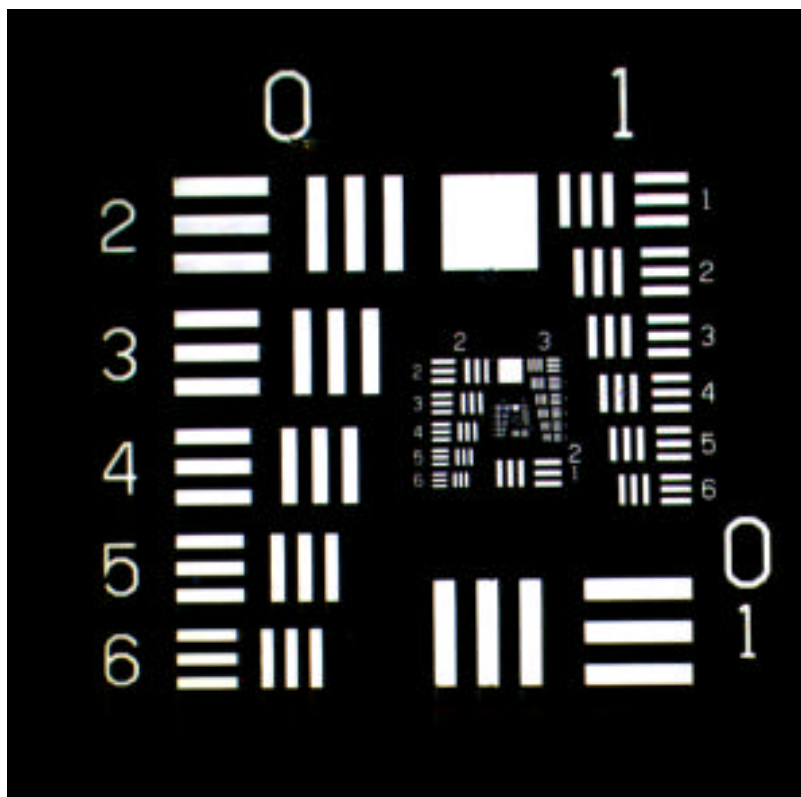
The effect of the chromatic aberration on the traditional system is more evident on closer inspection as shown in Figure 8.a. The decomposed view of the images show how poorly the red and green channels are focused while the blue channel is focused nicely. Figure 8.b shows the decomposed and composite images from the CPM system after post processing.

To see the results on a pixel level, Figure 9 shows a zoomed version of the number '3' in the upper right hand corner of the images in Figure 8. At a pixel level the chromatic aberration effects are dramatic. While it is possible to see the number '3' in the traditional system in Figure 9.a, the image is far from ideal due to the overwhelming chromatic misfocus of the red and green channels. The post processed CPM system image is clear even at such a close-up look. There is a sub-pixel shift that occurs due to slight tilt of

individual color filters, but these are corrected for by simple image processing. Notice the slight color traces in Figure 9.b of the CPM system image that arise from the still present lateral chromatic aberration. This can be corrected by choosing an optical system which is corrected for lateral chromatic aberration.



(a)



(b)

**Figure 7.** Images of entire resolution target with (a) traditional and (b) post processed CPM systems.

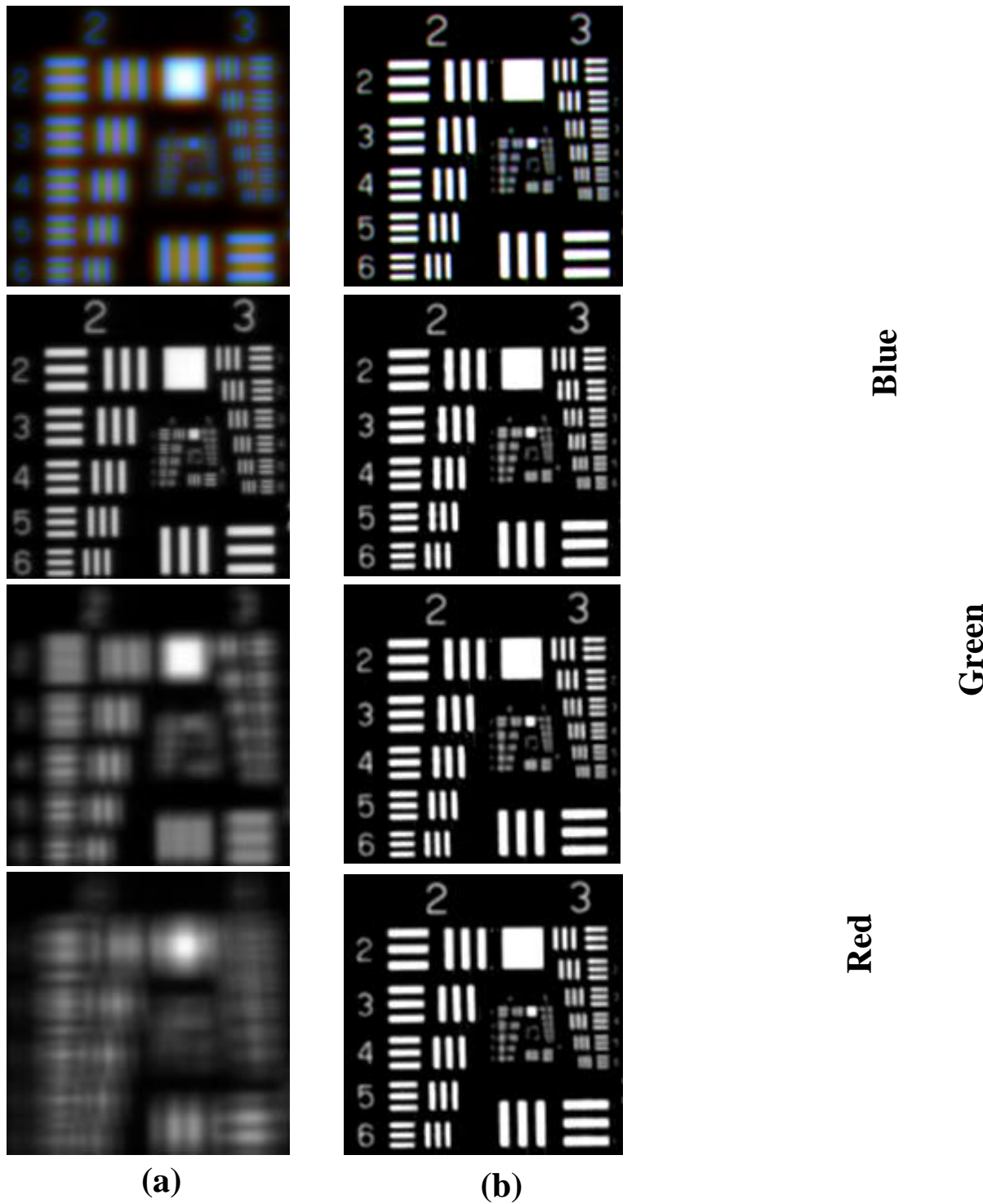


**Figure 8.** Portion of a resolution chart taken with a (a) traditional system and the (b) post processed CPM system. At the top are the three-color composite images and below are the individual color constituent images.

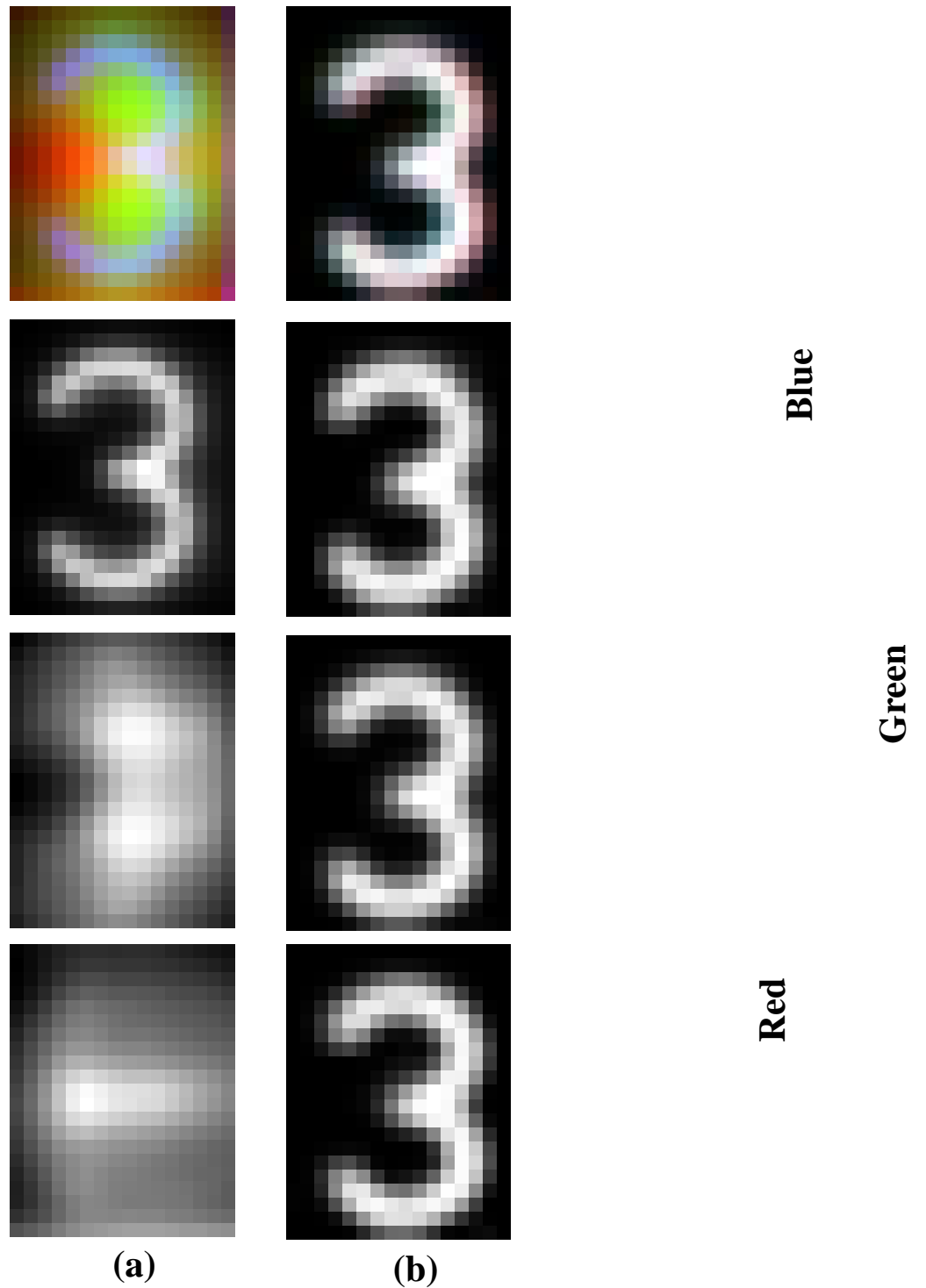


**Figure 9.** A very small portion of the resolution chart showing the effects of chromatic aberration on a pixel level. The traditional system composite image and constituent images are shown in (a) and those of the post processed CPM system shown in (b).

## **6. Conclusion**

Existing methods of achromatizing an optical system have limitations that may hinder the optimization of the system. As described in the introduction, most traditional achromatic systems require different lens media and then can only correct for a finite set of wavelengths. Hybrid refractive-diffractive optics have recently been used in achromatizing systems, but these elements also suffer from similar limitations. Here, a method has been developed for correcting axial chromatic aberration, over a large range of wavelengths. The optical-digital system employs a cubic phase modulation plate and digital post processing on the image. A fully achromatic system can be achieved by correcting the optical system for lateral chromatic aberration and leaving the axial chromatic aberration to the CPM plate and the digital post processing.

Sponsored in part by the Army Research office under grant number DAAG55-97-1-0348 and the Colorado Advanced Technology Institute. The information herein does not necessarily reflect the position of the federal government.

### **A1. Achromatizing a System**

The purpose of this appendix is to give a derivation of the contribution of a single thin lens element to chromatic aberration. Also, it will be shown how to correct for axial or lateral chromatic aberration with a single glass.

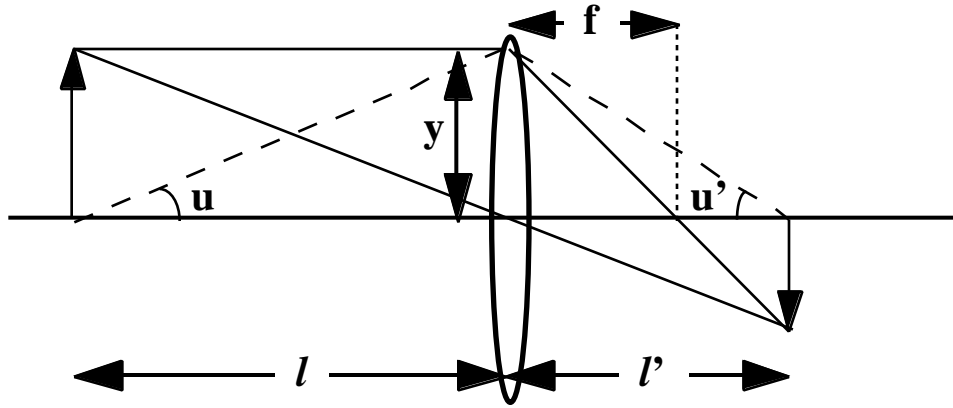


**Figure A1.1.** A single thin lens element with focal length  $f$ . The distance  $l$  is the object distance and the distance  $l'$  is the image distance. The ray height  $y$  is related to the ray angle  $u$  through the paraxial approximation  $y=lu=l'u'$ .

### Contribution of a Single Element to Axial Chromatic Aberration

The classical relation between object and image distance is

$$\frac{1}{l} - \frac{1}{l'} = (n - 1) \left( \frac{1}{R_1} - \frac{1}{R_2} \right) = (n - 1)c = \frac{1}{f} \quad (\text{A1.1})$$

where  $l$  is the object distance,  $l'$  is image distance and  $n$  is the index of refraction of the lens. The constant  $c$  is related to the radii of curvature of the lens surfaces  $R_1$  and  $R_2$ .

Writing (A1.1) for two wavelengths of light, F (blue) and C (red), and denoting their respective variables with the subscripts F and C, results in two relations between object and image distance. Subtracting these two relations gives

$$-\frac{1}{l_C} + \frac{1}{l_F} + \frac{1}{l_C} - \frac{1}{l_F} = (n_F - n_C)c$$

$$\frac{l_C - l_F}{l^2} - \frac{l_C - l_F}{l^2} = (n_F - n_C)c \frac{n_d - 1}{n_d - 1} = \frac{1}{fV} \quad (\text{A1.2})$$

where  $l^2 = l_C l_F$ ,  $l'^2 = l'_C l'_F$ , the focal length is  $f = \frac{1}{(n_d - 1)c}$  and the Abbe number is  $V = \frac{n_d - 1}{n_F - n_C}$ . The index of refraction  $n_d$  is representative of yellow light which is near the middle of the visible spectrum. Multiplying both sides by the negative ray height squared,  $-y^2$ , gives

$$L_{ch} \left( \frac{y^2}{l^2} \right) - L_{ch} \left( \frac{y^2}{l'^2} \right) = -\frac{y^2}{fV} \quad \text{or} \quad L_{ch}(u^2) - L_{ch}(u'^2) = -\frac{y^2}{fV} \quad (\text{A1.3})$$

where the ray angles  $u$  and  $u'$  are related to the ray height  $y$  through the paraxial approximation  $y = ul = u'l'$ .  $L_{ch}$  is the difference in object distance between the C and F light and  $L_{ch}$  is the difference in image distance between C and F light. For an achromatic lens, C and F light coming from the same object point must focus at the same image point so the left hand side of (A1.3) should be zero. It is now possible to see why a single thin lens cannot be achromatic. However, if more than one element are combined into a single system it is possible to create an achromatic lens. For the case where there are  $j$  elements (A1.3) becomes

$$L_{ch_j}(u_j^2) - L_{ch_j}(u_j'^2) = -\sum_{i=1}^j \frac{y_i^2}{f_i V_i} \quad (\text{A1.4})$$

Then to create an achromatic lens system it is necessary that the right hand side of (A1.4) is zero. Further, in an achromatic doublet using thin lenses the elements are in contact and therefore all of the  $y_i$ 's are equal and the necessary condition is reduced to

$$\frac{K_1}{V_1} + \frac{K_2}{V_2} = 0 \quad (\text{A1.5})$$

where  $K$  is the power or inverse focal length of a lens.

## Correcting Axial Chromatic Aberration with One Material

It is possible to correct for axial chromatic aberration with a dialyte (separated thin-lens achromat) using only one type of glass. Figure A1.2 shows a diagram of a dialyte. Two thin lenses, denoted (a) and (b), are separated by a distance  $d$  and have focal lengths  $f_a$  and  $f_b$  respectively. In order to correct axial chromatic aberration it is necessary to make the back focal lengths, for the wavelengths of interest, equal. That is, the distance behind lens (b) at which light of two different wavelengths focuses must be equal. In Figure A1.2 this distance is denoted  $l'$  and to simplify the analysis we use rays coming from infinity that are parallel to the optic axis and strike lenses (a) and (b) and heights  $y_a$  and  $y_b$  respectively.

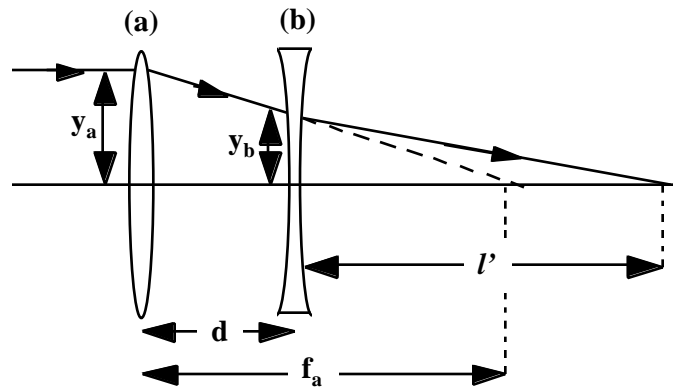


**Figure A1.2.** Two lenses, (a) and (b), separated by a distance  $d$  which are designed to correct for axial chromatic aberration, for two wavelengths, with the use of only one material. The lenses have focal lengths  $f_a$  and  $f_b$  and collimated light of two wavelengths focus at a distance  $l'$  behind lens (b).

For the system in Figure A1.2 to be axially achromatic the contributions of each lens element should add to zero. Substituting the lenses into (A1.4) and setting equal to zero gives

$$\frac{y_a^2}{f_a V_a} + \frac{y_b^2}{f_b V_b} = 0 \quad (\text{A1.6})$$

Also, with a little thought, figure A1.2 shows that  $y_b = y_a(f_a - d)/f_a = y_a(1 - d/f_a)$ .

Inserting this relation into (A1.6) gives

$$f_b V_b = -f_a V_a (1 - d/f_a)^2 \quad (\text{A1.7})$$

The effective focal length,  $F$ , of the system is related to the individual focal lengths and the spacing between the lenses by

$$\frac{1}{F} = \frac{1}{f_a} + \frac{1}{f_b} - \frac{d}{f_a f_b} = \frac{1}{f_a} + \frac{1 - d/f_a}{f_b} \quad (\text{A1.8})$$

The focal lengths of each lens can be found by combining (A1.7) and (A1.8) which produces

$$f_a = F \left( 1 - \frac{V_b}{V_a(1 - d/f_a)} \right) \quad \text{and} \quad f_b = F(1 - d/f_a) \left( 1 - \frac{V_a(1 - d/f_a)}{V_b} \right) \quad (\text{A1.9})$$

Now if we require that the two lenses be of the same material then we set  $V_a = V_b$  in (A1.9) which results in

$$f_a = \frac{Fd/f_a}{d/f_a - 1} \quad \text{and} \quad f_b = -Fd(d/f_a - 1)/f_a \quad (\text{A1.10})$$

Assuming collimated light, all of the rays incident on the first lens are parallel to the optic axis and therefore all the rays are focused to the point  $f_a$  behind the first lens. The object distance for the second lens is then  $f_a - d$ . We can then write the final image distance,  $l'$ , as

$$\frac{1}{l'} = \frac{1}{f_a - d} + \frac{1}{f_b}$$

Multiplying both sides by  $1-d/f_a$  gives

$$\frac{1}{l}(1-d/f_a) = \frac{1}{f_a} + \frac{1}{f_b}(1-d/f_a) = \frac{1}{F}$$

and the expression for the final image distance can be written as

$$l = F(1-d/f_a) = -F(d/f_a - 1) \quad (\text{A1.11})$$

An alternative method for arriving at this solution can be found in [4].

### Correcting Lateral Chromatic Aberration with One Material

It is also possible to correct two wavelengths for the lateral (or magnification) chromatic aberration using a single material. In order to accomplish this, it is necessary to set equal the effective focal lengths at the wavelengths of interest. Referring to Figure A1.2 and recalling the expression for the effective focal length in (A1.8) we can write the effective focal lengths for F (blue) and C (red) light,  $F_C$  and  $F_F$ .

$$\begin{aligned} \frac{1}{F_C} &= (n_{aC} - 1)c_a + (n_{bC} - 1)c_b - d(n_{aC} - 1)c_a(n_{bC} - 1)c_b \\ \frac{1}{F_F} &= (n_{aF} - 1)c_a + (n_{bF} - 1)c_b - d(n_{aF} - 1)c_a(n_{bF} - 1)c_b \end{aligned} \quad (\text{A1.12})$$

Here,  $c_z$  refers to the curvature of the  $z^{\text{th}}$  lens and  $n_{zy}$  is the index of refraction of the  $z^{\text{th}}$  lens at the wavelength  $y$ . We can set  $n_{aC} = n_{bC} = n_C$  and  $n_{aF} = n_{bF} = n_F$  since both lenses are made of the same material. Then equating the effective focal lengths yields,

$$(n_C - 1)[c_a + c_b - dc_a c_b(n_C - 1)] = (n_F - 1)[c_a + c_b - dc_a c_b(n_F - 1)]$$

Subtracting the right hand side out and combining some terms gives

$$(n_C - n_F)[c_a + c_b - dc_a c_b (n_C + n_F - 2)] = 0 \quad (\text{A1.13})$$

Multiply both top and bottom by  $n_d - 1$  and recall that the focal length can be written as

$$\frac{1}{f} = (n_d - 1)c \quad \text{and the Abbe number as } V = \frac{n_d - 1}{n_F - n_C}.$$

$$\frac{1}{V} \frac{1}{f_a} + \frac{1}{f_b} - \frac{dc_b}{f_a} \frac{n_d - 1}{n_d - 1} (n_C + n_F - 2) = 0$$

This expression can be simplified to

$$\frac{1}{V} \frac{1}{f_a} + \frac{1}{f_b} - \frac{d}{f_a f_b} \frac{n_C + n_F - 2}{n_d - 1} = 0 \quad (\text{A1.14})$$

Solving (A1.14) for  $d$  yields

$$d = \frac{1}{f_a} + \frac{1}{f_b} f_a f_b \frac{n_d - 1}{n_C + n_F - 2} \quad (\text{A1.15})$$

Now if we assume that  $n_d = \frac{n_C + n_F}{2}$  we can rewrite (A1.15) as

$$d = (f_a + f_b) \frac{n_C + n_F - 2}{n_C + n_F - 2} \frac{1}{2}$$

Further simplification gives our final result,

$$d = \frac{f_a + f_b}{2} \quad (\text{A1.16})$$

This is exactly the form of the Huygen's ocular in which lateral chromatic aberration is corrected with two singlet lenses of the same material by separating the lenses a distance equal to the average of their focal lengths. An alternative method for arriving at the above solution can be found in [4].

## **References**

- <sup>1</sup> Claude Tribastone, Charles Gardner and William G. Peck, "Precision plastic optics applications from design to assembly," in *Design, fabrication, and applications of precision plastic optics*, Xiaohui Ning, Raymond T. Hebert, ed., Proc. SPIE **2600**, pp. 6-9 (1995).
- <sup>2</sup> Pantazis Mouroulis and John Macdonald, *Geometrical Optics and Optical Design*, Oxford University Press, New York, 1997, pp.194-196.
- <sup>3</sup> R. Kingslake, *Lens Design Fundamentals*, Academic Press, New York, 1978, pp. 89-92.
- <sup>4</sup> Daniel Malacara and Zacarías Malacara, "Achromatic aberration correction with only one glass," in *Current developments in optical design and optical engineering IV*, Robert E. Fischer, Warren J. Smith, ed., Proc. SPIE **2263**, pp. 81-87 (1994).
- <sup>5</sup> Thomas Stone and Nicholas George, "Hybrid diffractive-refractive lenses and achromats," *Applied Optics*, Vol. 27, No. 14, pp.2960-2971.

- <sup>6</sup> K. Maruyama, M. Iwaki, S. Wakamiya and R. Ogawa, " A hybrid achromatic objective lens for optical data storage," in *International Conference on Applications of Optical Holography*, Toshio Honda, ed., Proc. SPIE **2577**, pp. 123-129 (1995).
- <sup>7</sup> K. Spaulding and G. M. Morris, "Achromatization of optical waveguide components using diffractive elements," in *Miniature and micro-optics : fabrication and system applications II*, Chandrasekhar Roychoudhuri, Wilfrid B. Veldkamp, ed., Proc. SPIE **1751**, pp. 225-228 (1992).
- <sup>8</sup> J. W. Goodman, *Introduction to Fourier Optics* (McGraw-Hill, New York, 1968), Chap. 6, pp. 120-125.
- <sup>9</sup> Edward R. Dowski, Jr. and W. Thomas Cathey, "Extended depth of field through wavefront coding," *Applied Optics*, Vol. 34 No. 11, pp. 1859-1866.
- <sup>10</sup> P.M. Woodward, *Probability and Information Theory with Applications to Radar*, Permagon, New York, 1953.